



HAL
open science

Spin–orbit interaction in the HD^+ ion

Vladimir I. Korobov, Jean-Philippe Karr

► **To cite this version:**

Vladimir I. Korobov, Jean-Philippe Karr. Spin–orbit interaction in the HD^+ ion. The European Physical Journal D: Atomic, molecular, optical and plasma physics, 2022, 76 (10), pp.197. 10.1140/epjd/s10053-022-00522-3 . hal-03826634

HAL Id: hal-03826634

<https://hal.science/hal-03826634>

Submitted on 24 Feb 2023

HAL is a multi-disciplinary open access archive for the deposit and dissemination of scientific research documents, whether they are published or not. The documents may come from teaching and research institutions in France or abroad, or from public or private research centers.

L'archive ouverte pluridisciplinaire **HAL**, est destinée au dépôt et à la diffusion de documents scientifiques de niveau recherche, publiés ou non, émanant des établissements d'enseignement et de recherche français ou étrangers, des laboratoires publics ou privés.

Spin-orbit interaction in the HD⁺ ion

Vladimir I. Korobov¹ and Jean-Philippe Karr^{2,3}

¹*Bogoliubov Laboratory of Theoretical Physics, Joint Institute for Nuclear Research, Dubna 141980, Russia*

²*Laboratoire Kastler Brossel, Sorbonne Université, CNRS, ENS-Université PSL,*

Collège de France, 4 place Jussieu, F-75005 Paris, France and

³*Université d'Evry-Val d'Essonne, Université Paris-Saclay, Boulevard François Mitterrand, F-91000 Evry, France*

We report on progress in calculation of the spin-orbit interaction for the HD⁺ molecular ion. This interaction is currently the largest source of theoretical uncertainty in determination of the hyperfine structure of rovibrational transition lines. The corrections of order $m\alpha^7 \ln(\alpha)$ are derived and numerically calculated. Theoretical hyperfine intervals are compared with experimental data, and the observed discrepancies are discussed.

In recent years several experiments [1–3] succeeded in measuring ro-vibrational transition lines in the HD⁺ molecular ion with relative precision of a few ppt. On the theoretical side, the "spin-averaged" transition energies were calculated with relative uncertainties of 1.4×10^{-11} for the pure rotational transition and of 7.5×10^{-12} for vibrational transitions [4, 5]. The main limitation in theoretical predictions comes from the hyperfine structure of transition lines [6], although in recent years there has been significant progress in the calculation of the hyperfine structure both in the $m\alpha^6$ order [7, 8] and in higher orders [9].

The main purpose of this work is to fill in the gap in the theory by calculating corrections of the order of $m\alpha^7 \ln(\alpha)$ to the spin-orbit interaction. This will allow to get theoretical predictions for the favored hyperfine components of a ro-vibrational transition (which keep the spin configuration of the molecular ion unchanged) without any significant loss of precision with respect to the spin-averaged transition energy.

I. NONRELATIVISTIC QED

In our derivation of the QED corrections to the hyperfine sublevels of the state we use the Nonrelativistic QED (NRQED) suggested in [10, 11]. The Lagrangian for the NRQED is expressed in terms of nonrelativistic (two-component) Pauli spinor fields ψ for each of the electron, positron, muon, proton, etc. Photons are treated in the same way as in QED. The Lagrangian is constrained by the natural symmetry requirements such as gauge invariance, hermiticity, time reversal symmetry, parity conservation, Galilean invariance and consequently the rotational invariance. The Coulomb gauge is used for the NRQED calculations.

Following [12] we use operators: $D_t = \partial_t + ieA_0$, $\mathbf{D} = \nabla - ie\mathbf{A}$, \mathbf{B} , \mathbf{E} , $\boldsymbol{\sigma}$, as building blocks of the Lagrangian and expand it into a series of inverse powers of the electron mass m :

$$\mathcal{L} = \sum_{n=0} \psi_f^* \frac{O_n}{m_e^n} \psi_e. \quad (1)$$

Spatial parity and time reversal symmetries of the operators are given in Table I.

Using symmetries imposed on the Lagrangian, one can show that the form of \mathcal{L} is **unique**, and the coefficients: c_F , c_D , etc. can be unambiguously obtained from a comparison with the scattering amplitude in QED after choosing the regularization in NRQED. The only arbitrariness is associated with the choice of a basis for homogeneous polynomials of \mathbf{p} , \mathbf{p}' (the electron impulse before and after scattering) to express the interactions in momentum space. Namely, for terms of degree 2, the interactions may be separated into $p^2 + p'^2$, $\mathbf{p}\mathbf{p}'$ or $(\mathbf{p} + \mathbf{p}')^2$, $(\mathbf{p} - \mathbf{p}')^2$.

With the help of these rules we arrive at the NRQED Hamiltonian expanded up to terms of $1/m^4$ order:

$$\begin{aligned} H_I = & eA_0 - c_F \frac{e}{2m} \boldsymbol{\sigma} \mathbf{B} - c_D \frac{e}{8m^2} [\nabla \mathbf{E}] + c_S \frac{e}{8m^2} \boldsymbol{\sigma} \cdot (\boldsymbol{\pi} \times \mathbf{E} - \mathbf{E} \times \boldsymbol{\pi}) \\ & + c_W \frac{e}{8m^3} \left\{ \boldsymbol{\pi}^2, \boldsymbol{\sigma} \mathbf{B} \right\} - c_{q^2} \frac{e}{8m^3} \boldsymbol{\sigma} \cdot [\Delta \mathbf{B}] + c_{p'p} \frac{e}{8m^3} \left\{ \boldsymbol{\pi} \cdot \mathbf{B} \boldsymbol{\sigma} \cdot \boldsymbol{\pi} \right\} \\ & + c_M \frac{e}{8m^3} \left(\boldsymbol{\pi} \cdot [\nabla \times \mathbf{B}] + [\nabla \times \mathbf{B}] \cdot \boldsymbol{\pi} \right) + c_A \frac{e^2}{8m^3} (\mathbf{E}^2 - \mathbf{B}^2) \\ & + c_{X_1} \frac{e}{128m^4} \left\{ \boldsymbol{\pi}^2, (\mathbf{D}\mathbf{E} + \mathbf{E}\mathbf{D}) \right\} + c_{X_2} \frac{e}{64m^4} \left\{ \boldsymbol{\pi}^2, [\nabla \mathbf{E}] \right\} - c_{X_3} \frac{e}{8m^4} \left[\Delta [\nabla \mathbf{E}] \right] \\ & - c_{Y_1} \frac{e}{64m^4} \left\{ \boldsymbol{\pi}^2, \boldsymbol{\sigma} \cdot (\boldsymbol{\pi} \times \mathbf{E} - \mathbf{E} \times \boldsymbol{\pi}) \right\} + c_{Y_2} \frac{ie}{4m^4} \epsilon_{ijk} \sigma^i \pi^j [\nabla \mathbf{E}] \pi^k, \end{aligned} \quad (2)$$

	$\boldsymbol{\pi}$	\mathbf{E}	\mathbf{B}	$\boldsymbol{\sigma}$
P	-	-	+	+
T	-	+	-	-
Dimension	M^1	M^2	M^2	M^0

TABLE I. Spatial parity and time reversal symmetries, and mass dimension of operators.

where $\boldsymbol{\pi} = -i\mathbf{D} = \mathbf{p} - e\mathbf{A}$, $\mathbf{E} = -\partial_t\mathbf{A} - \nabla A_0$, and $\mathbf{B} = \nabla \times \mathbf{A}$. Covariant derivatives in square brackets act only on the fields within the brackets. Similar results but in the Lagrangian form were obtained previously in [13] for terms up to $1/m^3$ order and in [14] including terms of order $1/m^4$.

The coefficients c_i are defined as follows:

$$\begin{aligned}
c_F &= 1 + a_e, & c_S &= 1 + 2a_e, & c_D &= 1 + 2a_e + \frac{\alpha}{\pi} \frac{8}{3} \left[\ln\left(\frac{m}{2\Lambda}\right) + \frac{5}{6} - \frac{3}{8} \right], \\
c_W &= 1, & c_{q^2} &= \frac{a_e}{2} + \frac{\alpha}{\pi} \frac{4}{3} \left[\ln\left(\frac{m}{2\Lambda}\right) + \frac{5}{6} - \frac{1}{8} \right], & c_{p'p} &= a_e, \\
c_M &= \frac{a_e}{2} + \frac{\alpha}{\pi} \frac{4}{3} \left[\ln\left(\frac{m}{2\Lambda}\right) + \frac{5}{6} - \frac{3}{8} \right], & c_A &= 1 + a_e, & & \\
c_{X_1} &= 5 + 4a_e, & c_{X_2} &= 3 + 4a_e, & c_{X_3} &= \frac{\alpha}{\pi} \left[\frac{11}{15} \ln\left(\frac{m}{2\Lambda}\right) + \frac{5}{6} - \frac{13}{40} \right], \\
c_{Y_1} &= 3 + 4a_e, & c_{Y_2} &= -\frac{\alpha}{\pi} \frac{1}{3} \left[\ln\left(\frac{m}{2\Lambda}\right) + \frac{5}{6} + \frac{1}{8} \right].
\end{aligned} \tag{3}$$

where a_e is the anomalous magnetic moment of an electron, $\Lambda \approx m\alpha^2$ is a cutoff parameter, which determines the upper limit of the photon momenta in the NRQED integrations.

When we are interested in calculating contributions only of order $m\alpha^7 \ln(\alpha)$, we may replace Λ by $m\alpha^2$ in the coefficients and ignore all higher order contributions, as in the following example:

$$c_{q^2} \Rightarrow \frac{\alpha}{\pi} \frac{4}{3} \ln(\alpha^{-2}), \quad \text{etc.}$$

II. ADVANCED HYPERFINE STRUCTURE THEORY OF HD^+

The effective spin Hamiltonian for the hyperfine splitting of a ro-vibrational state in the molecular ion HD^+ may be written in a form [15]:

$$\begin{aligned}
H_{\text{HFS}} &= E_1(\mathbf{L} \cdot \mathbf{s}_e) + E_2(\mathbf{L} \cdot \mathbf{I}_p) + E_3(\mathbf{L} \cdot \mathbf{I}_d) + E_4(\mathbf{I}_p \cdot \mathbf{s}_e) + E_5(\mathbf{I}_d \cdot \mathbf{s}_e) \\
&\quad + E_6 \left\{ 2\mathbf{L}^2(\mathbf{I}_p \cdot \mathbf{s}_e) - 3[(\mathbf{L} \cdot \mathbf{I}_p)(\mathbf{L} \cdot \mathbf{s}_e) + (\mathbf{L} \cdot \mathbf{s}_e)(\mathbf{L} \cdot \mathbf{I}_p)] \right\} \\
&\quad + E_7 \left\{ 2\mathbf{L}^2(\mathbf{I}_d \cdot \mathbf{s}_e) - 3[(\mathbf{L} \cdot \mathbf{I}_d)(\mathbf{L} \cdot \mathbf{s}_e) + (\mathbf{L} \cdot \mathbf{s}_e)(\mathbf{L} \cdot \mathbf{I}_d)] \right\} \\
&\quad + E_8 \left\{ 2\mathbf{L}^2(\mathbf{I}_p \cdot \mathbf{I}_d) - 3[(\mathbf{L} \cdot \mathbf{I}_p)(\mathbf{L} \cdot \mathbf{I}_d) + (\mathbf{L} \cdot \mathbf{I}_d)(\mathbf{L} \cdot \mathbf{I}_p)] \right\} \\
&\quad + E_9 \left[\mathbf{L}^2 \mathbf{I}_d^2 - \frac{3}{2}(\mathbf{L} \cdot \mathbf{I}_d) - 3(\mathbf{L} \cdot \mathbf{I}_d)^2 \right].
\end{aligned} \tag{4}$$

Couplings of the nuclear magnetic moments with the orbital magnetic field (coefficients E_2 , E_3 , and E_8), as well as the deuteron quadrupole moment coupling with the orbital part (E_9) are very small (see Table II). They can be treated perturbatively and their values calculated within the Breit-Pauli approximation as in [15] are sufficiently accurate for the present level of theoretical precision. Magnitude of other coefficients (in MHz) is also shown in the Table.

We use the coupling scheme for angular momentum operators: $\mathbf{F} = \mathbf{s}_e + \mathbf{I}_p$, $\mathbf{S} = \mathbf{F} + \mathbf{I}_d$, $\mathbf{J} = \mathbf{F} + \mathbf{L}$, which reflects (see Fig.1) the fact that the hyperfine structure is predominantly defined by the spin configuration of the system and interaction of the total spin \mathbf{S} with the total orbital angular momentum is the smallest coupling in the hyperfine splitting of a ro-vibrational level.

Coefficients E_4 and E_5 had been calculated in [9] with a relative uncertainty of about 10^{-6} . Coefficients E_6 and E_7 were obtained with account of the terms of $m\alpha^6$ order in [8]. Here we focus on the coefficient E_1 , which requires contributions of the order of $m\alpha^7 \ln(\alpha)$ to be taken into account.

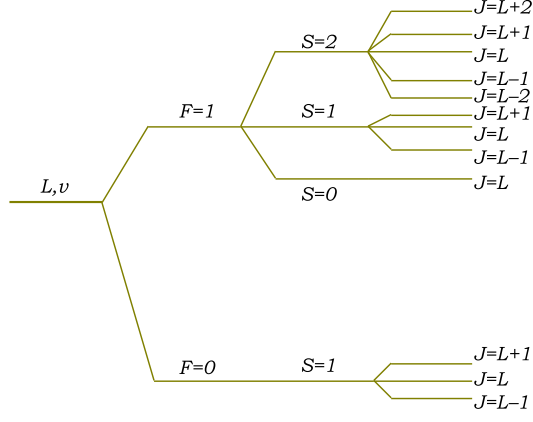


FIG. 1. Schematic diagram of the hyperfine splitting of a rovibrational state (L, v) of HD^+ .

E_1	E_2	E_3	E_4	E_5	E_6	E_7	E_8	E_9
31.9846	-3.134[-02]	-4.809[-03]	924.569	142.161	8.6111	1.3218	-3.057[-03]	5.666[-03]

TABLE II. Coefficients E_i of the effective spin Hamiltonian (in MHz) for the $(L=1, v=0)$ state (from [15]), $a[b] = a \times 10^b$.

A. Spin-orbit interaction

The leading-order $m\alpha^4$ relativistic corrections for the spin-orbit interaction is expressed [8]:

$$H_{so} = -c_F \left(\frac{Z_1}{mM_1} \frac{[\mathbf{r}_1 \times \mathbf{P}_1]}{r_1^3} + \frac{Z_2}{mM_2} \frac{[\mathbf{r}_2 \times \mathbf{P}_2]}{r_2^3} \right) \mathbf{s}_e + c_S \left(\frac{Z_1}{2m^2} \frac{[\mathbf{r}_1 \times \mathbf{p}_e]}{r_1^3} + \frac{Z_2}{2m^2} \frac{[\mathbf{r}_2 \times \mathbf{p}_e]}{r_2^3} \right) \mathbf{s}_e, \quad (5)$$

where coefficients c_F and c_S are defined as in Eq. (3), \mathbf{p}_e and \mathbf{P}_a are impulses of the electron and nuclei, correspondingly.

The effective Hamiltonian at $m\alpha^6$ and $m\alpha^7 \ln(\alpha)$ orders is derived from the NRQED Hamiltonian (2) in the same way as in [8], thus the spin-orbit interaction is expressed by a sum of the following operators:

$$H_{so}^{(6)} = c_W \mathcal{U}_W + c_{q^2} \mathcal{U}_{q^2} + c_{Y_1} \mathcal{U}_{Y_1} + c_{Y_2} \mathcal{U}_{Y_2} + c_S \mathcal{U}_{\text{CM}} + \mathcal{U}_{\text{MM}_N}, \quad (6)$$

where the first four operators are obtained from the tree-level contributions:

$$\begin{aligned} \mathcal{U}_W &= \frac{Z_1}{4m^3 M_1} \left\{ p_e^2, \frac{1}{r_1^3} [\mathbf{r}_1 \times \mathbf{P}_1] \right\} \mathbf{s}_e + \frac{Z_2}{4m^3 M_2} \left\{ p_e^2, \frac{1}{r_2^3} [\mathbf{r}_2 \times \mathbf{P}_2] \right\} \mathbf{s}_e, \\ \mathcal{U}_{q^2} &= \frac{iZ_1}{8m^3 M_1} \left\{ [\mathbf{p}_e \times (4\pi\delta(\mathbf{r}_1)) \mathbf{P}_1] \right\} \mathbf{s}_e + \frac{iZ_2}{8m^3 M_2} \left\{ [\mathbf{p}_e \times (4\pi\delta(\mathbf{r}_2)) \mathbf{P}_2] \right\} \mathbf{s}_e, \\ \mathcal{U}_{Y_1} &= -\frac{Z_1}{16m^4} \left\{ p_e^2, \frac{1}{r_1^3} [\mathbf{r}_1 \times \mathbf{p}_e] \right\} \mathbf{s}_e - \frac{Z_2}{16m^4} \left\{ p_e^2, \frac{1}{r_2^3} [\mathbf{r}_2 \times \mathbf{p}_e] \right\} \mathbf{s}_e, \\ \mathcal{U}_{Y_2} &= \frac{iZ_1}{2m^4} [\mathbf{p}_e \times (4\pi\delta(\mathbf{r}_1)) \mathbf{p}_e] \mathbf{s}_e + \frac{iZ_2}{2m^4} [\mathbf{p}_e \times (4\pi\delta(\mathbf{r}_2)) \mathbf{p}_e] \mathbf{s}_e, \end{aligned} \quad (7a)$$

while the last two are from the seagull-type diagrams:

$$\begin{aligned} \mathcal{U}_{\text{CM}} &= \frac{Z_1^2}{4m^2 M_1} \frac{1}{r_1^4} [\mathbf{r}_1 \times \mathbf{P}_1] \mathbf{s}_e + \frac{Z_2^2}{4m^2 M_2} \frac{1}{r_2^4} [\mathbf{r}_2 \times \mathbf{P}_2] \mathbf{s}_e \\ &\quad + \frac{Z_1 Z_2}{4m^2 M_1} \frac{1}{r_1 r_2^3} [\mathbf{r}_2 \times \mathbf{P}_1] \mathbf{s}_e + \frac{Z_1 Z_2}{4m^2 M_2} \frac{1}{r_1^3 r_2} [\mathbf{r}_1 \times \mathbf{P}_2] \mathbf{s}_e \\ &\quad - \frac{Z_1 Z_2}{4m^2 M_1} \frac{1}{r_1^3 r_2^3} [\mathbf{r}_1 \times \mathbf{r}_2] (\mathbf{r}_1 \mathbf{P}_1) \mathbf{s}_e + \frac{Z_1 Z_2}{4m^2 M_2} \frac{1}{r_1^3 r_2^3} [\mathbf{r}_1 \times \mathbf{r}_2] (\mathbf{r}_2 \mathbf{P}_2) \mathbf{s}_e, \\ \mathcal{U}_{\text{MM}_N} &= -\frac{Z_1^2}{2m^2 M_1} \frac{1}{r_1^4} [\mathbf{r}_1 \times \mathbf{p}_e] \mathbf{s}_e - \frac{Z_2^2}{2m^2 M_2} \frac{1}{r_2^4} [\mathbf{r}_2 \times \mathbf{p}_e] \mathbf{s}_e. \end{aligned} \quad (7b)$$

(1,0)	
$E_1^{(4)}$	31984.645
$E_1^{(6)}$	1.119
$E_1^{(7)}$	-0.347
E_1^{th}	31985.4(1)
E_1^{exp}	31984.9(1)

TABLE III. Contributions to the E_1 coefficient for the ($L=1, v=0$) state (in kHz).

The second-order perturbation contributions are expressed as follows:

$$\begin{aligned}
\Delta E_{so}^{2^{nd}\text{-order}} &= \Delta E_{so}^{(6)} + \Delta E_{so-ret} + \Delta E_{so-so}^{(1)} + \Delta E_{so}^{(7)}, \\
\Delta E_{so}^{(6)} &= 2 \left\langle H_{so} Q (E_0 - H_0)^{-1} Q H_B^{(4)} \right\rangle, \\
\Delta E_{so-ret} &= 2 \left\langle H_{so} Q (E_0 - H_0)^{-1} Q H_{ret} \right\rangle, \\
\Delta E_{so-so}^{(1)} &= \left\langle H_{so} Q (E_0 - H_0)^{-1} Q H_{so} \right\rangle^{(1)}, \\
\Delta E_{so}^{(7)} &= 2 \left\langle H_{so} Q (E_0 - H_0)^{-1} Q H_B^{(5)} \right\rangle.
\end{aligned} \tag{8}$$

Here we include into the Breit-Pauli Hamiltonian radiative corrections (as contribution to the Darwin coefficient, c_D , of Eq. (2)):

$$\begin{aligned}
H_B &= -\frac{p^4}{8m^3} + c_D \frac{\pi\alpha}{2m^2} [Z_1\delta(\mathbf{r}_1) + Z_2\delta(\mathbf{r}_2)] = \left\{ -\frac{p^4}{8m^3} + \frac{\pi\alpha}{2m^2} [Z_1\delta(\mathbf{r}_1) + Z_2\delta(\mathbf{r}_2)] \right\} \\
&\quad + \left(\frac{\alpha}{\pi} \frac{8}{3} \ln \alpha^{-2} \right) \frac{\pi\alpha}{2m^2} [Z_1\delta(\mathbf{r}_1) + Z_2\delta(\mathbf{r}_2)] = H_B^{(4)} + H_B^{(5)}.
\end{aligned}$$

It is worth noting that both first and second-order terms are finite and do not require regularization.

III. RESULTS

A. Pure rotational transition

In case of the pure rotational transition [1]: ($L=0, v=0$) \rightarrow ($L'=1, v'=0$), the hyperfine splitting is essentially larger relative to the transition line frequency magnitude than in the case of vibrational transitions. Using the six measured transition lines one can extract the experimental value of the E_1 coefficient. To do this, we fixed the coefficients of the effective HFS Hamiltonian (4), taking the best theoretical values for E_i , and then fit either two parameters: $f_{\text{spin-avg}}$ and E_1 , the spin-averaged transition frequency and the spin-orbit coupling coefficient, or four parameters: $f_{\text{spin-avg}}$, E_1 , E_6 , and E_7 . Results obtained by both methods agree well with each other and provide the following numbers:

$$f_{\text{spin-avg}}^{(\text{exp})} = 1\,314\,925\,752.905(10)_{\text{fit}}(17)_{\text{exp}} \text{ kHz},$$

and

$$E_1^{\text{exp}} = 31984.9(1) \text{ kHz}.$$

Results of the numerical calculations for the spin-orbit coupling coefficient are presented in Table III. From comparison with experimental fit one may see that there is some disagreement between theory and experiment of about 5σ . Thus we see that there is room for further careful study of this transition both in theory and experiment.

B. Two-photon vibrational transition

In case of the two-photon vibrational transition: ($L=3, v=0$) \rightarrow ($L'=3, v'=9$), the two following lines were measured [2]: f_0^{HF} : ($F=0, S=1, J=4$) \rightarrow ($F'=0, S'=1, J'=4$), and f_1^{HF} : ($F=1, S=2, J=5$) \rightarrow ($F'=1, S'=2, J'=5$)

	(3,0)	(3,9)
$E_1^{(4)}$	31627.352	18270.577
$E_1^{(6)}$	1.093	0.488
$E_1^{(7)}$	-0.341	-0.184
E_1	31628.1(1)	18270.9(1)

TABLE IV. Contributions to the E_1 coefficient for the ($L=3, v=0$) and (3,9) states (in kHz).

$f_{10,theo}^{HF}$	178 245.9(0.3)
$f_{10,exp}^{HF}$	178 254.4(0.9)

TABLE V. Comparison of the HFS interval f_{10} with the experiment.

5). The hyperfine splitting relative to the transition frequency is smaller, so that a precision of five significant digits in the coefficients of the effective HFS Hamiltonian (4) already allows to get a smaller absolute theoretical uncertainty than that of the spin-averaged transition frequency.

Table IV summarizes the contributions to the E_1 coefficient both for the initial (3,0) and final (3,9) states. Our final prediction for the $f_{10}^{HF} = f_0^{HF} - f_1^{HF}$ splitting (see Table V) confirms our previous conclusion [8] concerning the disagreement between theory and experiment with a deviation of about 9σ .

C. Conclusions

In summary, let us formulate the main theoretical results in the hyperfine structure calculations of the HD^+ molecular ion that were obtained in recent years:

- The spin-spin scalar interaction coefficients (E_4 and E_5) are now available with relative precision of $\sim 10^{-6}$ [9].
- The spin-orbit coefficient E_1 is obtained with corrections up to $m\alpha^7 \ln(\alpha)$ order (this work).
- The spin-spin tensor coefficients E_6 and E_7 have been obtained up to $m\alpha^6$ order. Improved numerical results for these coefficients will be presented in a forthcoming publication.
- Other HFS interactions (not included into the effective HFS Hamiltonian (4)) were also studied, particularly the nuclear spin-spin interaction mediated by the electron spin [16]. It is found [6] that this correction is too small to explain the observed discrepancies.

In a view of these achievements, it can be stated that the favored hyperfine components of ro-vibration transition lines can now be obtained with a theoretical precision that is mainly limited by the calculation of the spin-averaged transition frequency, i.e., 1.4×10^{-11} for pure rotational transitions and 7.5×10^{-12} for vibrational transitions. The main sources of theoretical uncertainty are the $m\alpha^8$ order one- and two-loop contributions to the spin-averaged transition frequency [4, 5].

D. Acknowledgements

This work was done in collaboration with Laurent Hilico, Mohammad Haidar (LKB), and Zhen-Xiang Zhong (Wuhan, WIPM CAS) that is gratefully acknowledged.

-
- [1] S. Alighanbari, G.S. Giri, F.L. Constantin, V.I. Korobov, and S. Schiller, Precise test of quantum electrodynamics and determination of fundamental constants with HD^+ ions, *Nature* **581**, 152 (2020).
- [2] S. Patra, M. Germann, J.-Ph. Karr, M. Haidar, L. Hilico, V. I. Korobov, F. M. J. Cozijn, K. S. E. Eikema, W. Ubachs, and J. C. J. Koelemeij, Proton-electron mass ratio from laser spectroscopy of HD^+ at the part-per-trillion level, *Science* **369**, 1238 (2020).

- [3] I. Kortunov, S. Alighanbari, M.G. Hansen, G.S. Giri, S. Schiller, and V.I. Korobov, Proton-electron mass ratio by high-resolution optical spectroscopy of ion ensemble in the resolved-carrier regime. *Nature Phys.* **17**, 569 (2021).
- [4] V.I. Korobov, L. Hilico, and J.-Ph. Karr, Fundamental transitions and ionization energies of the hydrogen molecular ions with few ppt uncertainty. *Phys. Rev. Lett.* **118**, 233001 (2017).
- [5] V.I. Korobov and J.-Ph. Karr, Rovibrational spin-averaged transitions in the hydrogen molecular ions, *Phys. Rev. A* **104**, 032806 (2021).
- [6] V.I. Korobov, Precision Spectroscopy of the Hydrogen Molecular Ions: Present Status of Theory and Experiment. *Physics of Particles and Nuclei*, **53**, 787–789 (2022).
- [7] M. Haidar, Z.-X. Zhong, V.I. Korobov and J.-Ph. Karr, NRQED approach to the fine and hyperfine structure corrections of order $m\alpha^6$ and $m\alpha^6(m/M)$: Application to the hydrogen atom. *Phys. Rev. A* **101**, 022501 (2020).
- [8] V.I. Korobov, J.-Ph. Karr, M. Haidar, and Zhen-Xiang Zhong, Hyperfine structure in the H_2^+ and HD^+ molecular ions at $m\alpha^6$ order. *Phys Rev. A* **102**, 022804 (2020).
- [9] J.-Ph. Karr, M. Haidar, L. Hilico, Zhen-Xiang Zhong, and V.I. Korobov, Higher-order corrections to spin-spin scalar interactions in HD^+ and H_2^+ . *Phys. Rev. A* **102**, 052827 (2020).
- [10] W.E. Caswell and G.P. Lepage, Effective Lagrangians for bound state problems in QED, QCD, and other field theories. *Phys. Lett. B* **167**, 437 (1986).
- [11] T. Kinoshita and M. Nio, Radiative corrections to the muonium hyperfine structure: The $\alpha^2(Z\alpha)$ correction. *Phys. Rev. D* **53**, 4909 (1996).
- [12] G. Paz, An introduction to NRQED. *Mod. Phys. Lett. A* **80**, 1550128 (2015).
- [13] A.V. Manohar, Heavy quark effective theory and nonrelativistic QCD Lagrangian to order a_s/m^3 . *Phys. Rev. D* **56**, 230 (1997).
- [14] R.J. Hill, G. Lee, G. Paz, and M.P. Solon, NRQED Lagrangian at order $1/M^4$. *Phys. Rev. D* **87**, 053017 (2013).
- [15] D. Bakalov, V.I. Korobov, and S. Schiller, High-precision calculation of the hyperfine structure of the HD^+ ion, *Phys. Rev. Lett.* **97**, 243001 (2006).
- [16] N. Ramsey, Electron Coupled Interaction Between Nuclear Spins in Molecule. *Phys. Rev.* **91**, 303 (1953).